ORIGINAL ARTICLE

JBMR®

The Proteasome Inhibitor Bortezomib Maintains Osteocyte Viability in Multiple Myeloma Patients by Reducing Both Apoptosis and Autophagy: A New Function for Proteasome Inhibitors

Denise Toscani,[1*] Carla Palumbo,[2*] Benedetta Dalla Palma,[1,3] Marzia Ferretti,[2] Marina Bolzoni,[1] Valentina Marchica,[1] Paola Sena,[2] Eugenia Martella,[4] Cristina Mancini,[4] Valentina Ferri,[1,5] Federica Costa,[1] Fabrizio Accardi,[1,3] Luisa Craviotto,[1] Franco Aversa,[1,3] and Nicola Giuliani[1,3]

[1]Myeloma Unit, Department of Clinical and Experimental Medicine, University of Parma, Parma, Italy
[2]Department of Biomedical, Metabolic, and Neural Sciences, Section of Human Morphology, University of Modena and Reggio Emilia, Modena, Italy
[3]Hematology Unit, "Azienda Ospedaliero-Universitaria di Parma", Parma, Italy
[4]Pathology, "Azienda Ospedaliero-Universitaria di Parma", Parma, Italy
[5]Department of Biotechnology and Life Sciences, University of Insubria, Varese, Italy

ABSTRACT

Multiple myeloma (MM) is characterized by severely imbalanced bone remodeling. In this study, we investigated the potential effect of proteasome inhibitors (PIs), a class of drugs known to stimulate bone formation, on the mechanisms involved in osteocyte death induced by MM cells. First, we performed a histological analysis of osteocyte viability on bone biopsies on a cohort of 37 MM patients with symptomatic disease. A significantly higher number of viable osteocytes was detected in patients treated with a bortezomib (BOR)-based regimen compared with those treated without BOR. Interestingly, both osteocyte autophagy and apoptosis were affected in vivo by BOR treatment. Thereafter, we checked the in vitro effect of BOR to understand the mechanisms whereby BOR maintains osteocyte viability in bone from MM patients. We found that osteocyte and preosteocyte autophagic death was triggered during coculturing with MM cells. Our evaluation was conducted by analyzing either autophagy markers microtubule-associated protein light chain 3 beta (LC3B) and SQSTM1/sequestome 1 (p62) levels, or the cell ultrastructure by transmission electron microscopy. PIs were found to increase the basal levels of LC3 expression in the osteocytes while blunting the myeloma-induced osteocyte death. PIs also reduced the autophagic death of osteocytes induced by high-dose dexamethasone (DEX) and potentiated the anabolic effect of PTH(1-34). Our data identify osteocyte autophagy as a new potential target in MM bone disease and support the use of PIs to maintain osteocyte viability and improve bone integrity in MM patients. © 2015 American Society for Bone and Mineral Research.

KEY WORDS: OSTEOCYTES; CANCER-INDUCED BONE DISEASE; MULTIPLE MYELOMA; PROTEASOME INHIBITORS; AUTOPHAGY

Introduction

Multiple myeloma (MM) is a plasma cell malignancy characterized by severely imbalanced and uncoupled bone remodeling in the bone marrow (BM) resulting from increased osteoclast formation and activity and osteoblast suppression.[1,2] Multiple osteolytic lesions occur in close proximity to the area of MM cell infiltration, rather than resulting from the production of soluble factors acting systematically.[1,2]

Recently, it has been shown that an increased osteocyte death occurs in MM patients with bone disease. Osteocytes, which are terminally differentiated cells derived from osteoblasts, are involved in bone remodeling both through cell death, which upregulates osteoclast recruitment, and by secreting sclerostin (SOST), a bone formation inhibitor.[3–8] Moreover, they express specific markers involved in mineralization and phosphate metabolism such as dentin matrix protein 1 (*DMP1*), a phosphate-regulating gene with homologies to endopeptidase on the X chromosome (*PHEX*), and fibroblast growth factor 23 (*FGF23*).[9] An increased osteocyte cell death is associated with osteoporosis caused by estrogen deficiency or glucocorticoid administration.[10–13] This leads to a reduction in the bone mineral

Received in original form May 28, 2015; revised form November 6, 2015; accepted November 8, 2015. Accepted manuscript online Month 00, 2015.
Address correspondence to: Nicola Giuliani, MD, PhD, Department of Clinical and Experimental Medicine, Myeloma Unit, University of Parma, Via Gramsci 14, 43126, Parma, Italy. E-mail: nicola.giuliani@unipr.it
*DT and CP contributed equally to this work.
Additional Supporting Information may be found in the online version of this article.
Journal of Bone and Mineral Research, Vol. 30, No. xx, Month 2015, pp 1–13
DOI: 10.1002/jbmr.2741

density with a prolonged life span of osteoclasts.[14–16] In the case of mice, the administration of intermittent PTH(1-34) or short-term exposure to PTH(1-34) has shown prolonged osteocyte survival with decreased osteoblast apoptosis.[17–19] Zoledronic acid (ZOL), used in MM patients to block osteoclast formation, also inhibits osteocyte death and apoptosis.[20,21] Recent data suggest that osteocytes can undergo a tightly regulated process of self-degradation called autophagy,[22,23] a pro-survival mechanism protecting from oxidative stress stimuli or aging.[24,25] However, under acute stress conditions, autophagy can be an unregulated self-destructive process leading to cell death independently of apoptosis.[4,23,24] Dexamethasone (DEX) treatment, both in vitro and in vivo, was consistently shown to increase the expression of the autophagy marker microtubule-associated protein light chain 3 beta (LC3B) in osteocytes,[26,27] leading to the possibility that an increased autophagic death might be involved in bone loss in patients receiving glucocorticoid therapy, such as MM patients. Recently, we demonstrated that the presence of bone lesions in MM patients was associated with a significantly reduced number of viable osteocytes.[28] An ultrastructural in vitro analysis on osteocytes cocultured with MM cells, showing a significant increase in osteocyte death, confirmed our observations.[28] Among the new drugs used in the treatment of MM, proteasome inhibitors (PIs), including bortezomib (BOR), affect bone remodeling by stimulating osteoblast differentiation in both mouse and human systems.[29,30] Moreover, recent studies have shown a significant increase in markers of osteoblast activity, such as alkaline phosphatase and osteocalcin, in MM patients treated with BOR.[31–34] The potential effects of PIs on osteocytes are not known, although they have been evaluated in this study. First, we evaluated osteocyte viability, autophagy, and apoptosis in the bone biopsies of MM patients who underwent different therapeutic regimens including BOR; second, the in vitro effects of PIs on osteocytes were evaluated in two different models of MM-induced osteocyte death[28] and DEX-induced osteocyte death.[13,14,26,27] Furthermore, the role of autophagy and apoptosis and the effects of PIs were investigated in those models, using both the human preosteocytic cell line HOB-01[35] and the murine osteocytic MLO-Y4.[36,37]

Materials and Methods

Ex vivo histological evaluations of osteocyte viability on bone biopsies of MM patients

A histological retrospective analysis of bone biopsies was performed on a cohort of 37 patients (15 females and 22 males) with monoclonal gammopathies. Thirty-one of them presented with symptomatic MM and six with smoldering MM (SMM). Bone biopsies were obtained from the iliac crest in both symptomatic MM and SMM patients, at the time of diagnosis and after, on average, 12 months of treatment/observation, respectively. The study was approved by our local Ethics Committee. All patients provided written informed consent in accordance with the Declaration of Helsinki. Cylindrical iliac biopsies (3 mm in diameter, 10 mm in length) were obtained from the patients, fixed in sodium phosphate-buffered 4% paraformaldehyde at pH 7.4, dehydrated in a graded series of ethanol, and embedded in paraffin. Bone samples were longitudinally sectioned by means of a microtome cutting system (Leica S.p.A., Milan, Italy) to obtain 5-micron-thick sections, and then stained with Gomori's trichrome stain (Polysciences, Inc., Eppelheim, Germany). Osteocyte viability was evaluated in a total of 500 lacunae per histological section, and two groups of data were collected: 1) the number of viable osteocytes and 2) the number of nonviable osteocytes (including degenerated osteocytes, apoptotic osteocytes, empty lacunae, and micropetrotic lacunae). Preliminary to the count collection, all sections were carefully observed under light microscopy, and it emerges that osteocyte viability appeared uniformly distributed throughout each section. Most of the sections contained about 500 lacunae; in the few sections containing less than 500 lacunae, osteocyte viability was evaluated in all lacunae; in the sections containing more than 500 lacunae, the considered 500 lacunae were randomly included in the counting, given that we did not observe areas with mostly viable osteocytes as well as areas with mostly nonviable osteocytes. The sections were observed and analyzed using a light microscope (Zeiss Axiophot, Jena, Germany), equipped with an image analysis system at 40× magnification (a Nikon DS-5Mc camera connected to a personal computer NIS Elements AR 2.20 Nikon software, Nikon Inc., Melville, NY, USA). The bone biopsy sections taken from 26 of 31 symptomatic MM patients also underwent in situ end-labeling analysis (TUNEL) for the evaluation of the amount of osteocyte apoptosis, using the ApopTag peroxidase in situ apoptosis kit (Millipore, Billerica, MA, USA) (counterstain Fast Green). Finally, in 25 of 31 bone sections obtained from symptomatic MM patients, MAP LC3 expression was assessed by immunofluorescence and evaluated using confocal microscopy as described below.

Statistical analysis was performed using nonparametric tests to compare median values of viable osteocytes across different groups of patients. A nonparametric multiple regression analysis was also performed to assess the impact of each treatment alternative on osteocyte viability.

Drugs

BOR was purchased from Janssen-Cilag (Milan, Italy). The drug was reconstituted in water at a stock concentration of 2.6 mM and diluted in the cell culture medium before use. Proteasome inhibitor Z-(Leu-Leu-Leu-B(OH)2) (MG 262) and caspase-3 inhibitor Ac-Asp-Glu-Val-Asp-CHO (Ac-DEVD-CHO) were purchased from Enzo Life Sciences (Florence, Italy). DEX was purchased from Sigma-Aldrich (Milan, Italy). Human PTH (1-34), chloroquine (CQ), and 3-methiladenine (3-MA) were purchased from Tocris Bioscience (Bristol, UK).

Cells and cell culture conditions

Cell lines

The human myeloma cell line (HMCL) JJN3 was purchased from DSMZ (Braunschweig, Germany) and HMCL RPMI 8226 from the American Type Culture Collection (Rockville, MD, USA). The pre-B acute lymphoblastic leukemia cell line 697 was kindly provided by Dr Irma Airoldi (Genoa, Italy). The human preosteocytic cells HOB-01 were established from human bone and kindly provided by Julia Billars (Collegeville, PA, USA). The murine osteocytic cells MLO-Y4 were kindly provided by Linda Bonewald (Kansas City, MO, USA). All cell lines were authenticated and tested for mycoplasma contamination.

Cell conditions and experimental procedures

Cells were cultured in a phenol red-free medium supplemented with 10% fetal bovine serum (FBS), 100 U/mL of penicillin, and

100 μg/mL of streptomycin. Confluent HOB-01 and MLO-Y4 cells were treated in 96-well plates for 12-24-48 hours with BOR (2-5-10 nM), or MG 262 (10 nM) or vehicle. In another set of experiments, we tested the different amounts of 48-hour conditioned media (CM) of HMCL RPMI 8226 to determine osteocyte viability and autophagy induction as reported in Supplemental Fig. S1*A, B*. For the subsequent experiments, we used the undiluted CM (100%). The confluent HOB-01 and MLO-Y4 cells were incubated in 96-well plates or 24-well plates in the presence (100%) or the absence (0%) of 48-hour CM of HMCLs RPMI 8226 and JJN3 or treated with DEX or vehicle at 10^{-6} M for 48 hours. Subsequently, the culture media was changed and the cells were treated for 12-24-48 hours with BOR (2–5 nM) or MG 262 (10 nM) or vehicle. In other series of experiments, MLO-Y4 were incubated with DEX or vehicle 10^{-5} M for 6 or 24 hours. Then the culture media was changed and the cells treated with PTH (1-34) (10 nM) for 1 hour or BOR (2nM) for 12 hours or PTH(1-34) (1 hour) followed by BOR (12 hours) or vehicle.

Cocultures

HOB-01 and MLO-Y4 cells were cocultured with HMCLs RPMI 8226 and JJN3 in a transwell insert for 48 hours. Then the culture medium was changed and the cells were treated for 12 hours with BOR (2 nM) or MG 262 (10 nM) or vehicles. In addition, both osteocytic cell lines were cocultured with lymphoblastic leukemia cell line 697 for 48 hours in a transwell insert. All pellets from the experiments were collected for cell viability, caspase-3 activity, Western blot, immunofluorescent confocal microscopy, and transmission electron microscopy.

Autophagy and apoptosis inhibition

MLO-Y4 cells were incubated in the presence or absence of 48-hour CM of RPMI 8226 or treated with DEX or vehicle at 10^{-6} M for 48 hours. 3-MA (0.5 mM), CQ (25 μM), Ac-DEVD-CHO (50 nM), or vehicles (dimethyl sulfoxide and water) were added 1 hour before induction of cell death and maintained throughout the culture period.

Osteocyte viability

Osteocyte viability was evaluated using a cytotoxicity assay, following manufacturer's protocol (Cell Counting Kit-8; Alexis Biochemicals, Plymouth Meeting, PA, USA). All experiments were performed in culture media supplemented with 5% FBS. Osteocyte viability in cocultures was evaluated by Trypan blue staining (Sigma-Aldrich).

Briefly, nonadherent cells and adherent cells released after trypsinization were combined and collected by centrifugation. Subsequently, 0.04% trypan blue was added, and both viable and dead or dying cells were determined using a Neubauer hemocytometer. At least 100 cells per condition were counted under the light microscope. The percentage of nonviable cells exhibiting intracellular staining per total cell number was calculated in each case.

Caspase-3 activity assay

To evaluate caspase-3 activity, nonadherent and adherent cells were harvested, combined, and assayed using a commercial kit (Caspase-3 Colorimetric Activity Assay kit, Millipore), following manufacturer's instructions. Quantification was performed using a spectrophotometer at 405 nm. All results are expressed as the mean value ± standard deviation (SD), and the mean values of the groups were compared using two-tailed Student's *t* test.

RNA isolation and real-time quantitative PCR

Total RNA was extracted from the cells using the RNeasy Total RNA Isolation Kit (Qiagen, Valencia, CA, USA) and then quantified using a Nanodrop ND-100 (Celbio S.p.A., Milan, Italy). One microgram of RNA was reverse transcribed with 400 U Moloney murine leukemia reverse transcriptase (Applied Biosciences, Life Sciences, Carlsbad, CA, USA) following manufacturer's protocol. Real-time PCR was performed using the TaqMan Gene Expression Assay (Applied Biosystems, Life Technologies, Milan, Italy) for the following genes:

FGF23: Hs00221003_m1; Mm00445621_m1, DMP1: Hs00189 368_m1; Mm01208363_m1, PHEX2: Hs01011692_m1; Mm0116 6563_m1, SOST: Hs00228830_m1; Mm00470479_m1.

PCR amplifications were run in duplicate on the LightCycler 480 (Roche Diagnostics, Milan, Italy). The Ct method was applied to normalize differences in the quantity and quality of RNA, and mRNA was quantified using comparative ΔCt method and the endogenous reference genes GAPDH (HOB-01) or β2-Microglobulin (MLO-Y4) (DCt¼mean Ct gene–mean Ct GAPDH/β2-Microglobulin). ΔΔCt was evaluated as the difference between the ΔCt value of a target sample and the ΔCt for the corresponding control sample. The fold change in mRNA expression was calculated as $2^{-\Delta\Delta Ct.}$

Western blot analysis

Total and cytosolic extracts were obtained using a commercial kit (Active Motif, Carlsbad, CA, USA). The following antibodies were used for immunoblotting: rabbit polyclonal anti-LC3 antibody (1:1000) (Code n.PD014, MBL International Corporation, Woburn, MA, USA), mouse anti-p62/SQSTM1 antibody (1:250) (Code n.MAB8028, R&D Systems, Minneapolis, MN, USA), and mouse anti-β-actin monoclonal antibody (1:5000) (Code n. A5441, Sigma-Aldrich) as an internal control. Anti-rabbit (1:2000) (Code n.7074, Chemicon, Temecula, CA, USA) and anti-mouse (1:10,000) (Code n.103001, BD Pharmingen, Franklin Lakes, NJ, USA) antibodies were used as peroxidase-conjugated secondary antibodies. Chemiluminescence was detected using luminol solution (ECL Plus, GE Healthcare Amersham, Milan, Italy). Immunoreactive bands were visualized with an exposure time of 15 minutes (Kodak XOMAT). LC3 conversion from LC3 form I (LC3-I, 18 kDa) to LC3 form II (LC3-II, 16 kDa), normalized by β-actin level, was our reported autophagy index.

Immunofluorescence confocal microscopy

Immunofluorescence analysis was carried out to assess the expression of MAP LC3 in bone biopsies and LC3 and Apaf-1 in the cell cultures. MLO-Y4 cells, cultured in different conditions in multiwell chamber slides, and bone biopsy samples were treated and observed as previously described.[38] Samples were incubated with the following antibodies: rabbit anti-MAP LC3 (Code n. sc-134226), mouse anti-Apaf-1 (Code n. sc-135836, Santa Cruz Biotechnology, Inc., Dallas, TX, USA); goat anti-rabbit Cy3 (Code n. C2306) and sheep anti-mouse FITC (Code n. F2883, Sigma-Aldrich). After being washed, samples were counterstained with 1 g/mL DAPI (4′,6-diamidin-2-fenilindolo) and then mounted with an anti-fade medium (0.21M DABCO (1,4-diazabicyclo[2.2.2] octane) and 90% glycerol in 0.02 M Tris (tris[hydroxymethyl]

aminomethane, pH 8.0). The negative control samples were not incubated with the primary antibody. The confocal imaging was performed on a Leica TCS SP2 AOBS confocal laser scanning microscope (Leica S.p.A.). To quantify MAP LC3-positive cells, 5 to 6 slides were examined at 40× magnification for each condition, in order to count almost 1000 cells as previously described.[38] All results are expressed as the mean % ±SD. The mean values of the groups were compared using ANOVA, followed by Bonferroni and Student-Newman-Keuls tests.

Transmission electron microscopy (TEM)

At the end of the culture period, monolayers of MLO-Y4 cells were fixed for 20 minutes in 4% paraformaldehyde in a 0.13 M phosphate buffer (pH 7.4), post-fixed for 20 minutes in 1% osmium tetroxide in a 0.13 M phosphate buffer (pH 7.4), dehydrated in graded ethanol, and embedded in epoxy resin (Durcupan ACM, SPI Supplies, Jeol-Italia, Milan, Italy). Then they were sectioned with a diamond knife mounted on an Ultracut-Reichert Microtome (Leica, Wetzlar, Germany). The ultrathin sections (70–80 nm) were mounted on Formvar/carbon-coated copper grids, stained with 1% uranyl acetate and lead citrate, and examined by means of a Zeiss EM109 transmission electron microscope (Zeiss AG, Jena, Germany).

Results

Increase of viable osteocytes in MM patients treated with BOR-based regimens

We retrospectively analyzed bone biopsies of 37 patients, 31 of which with symptomatic MM (19 newly diagnosed and 12 relapsed; International Staging System (ISS) (I–III: I = 3, II = 17, III = 11) and 6 with SMM (mean age ± SD of patients 68 ± 10 years; median age 68 years; range 35–88 years). A total of 73% of MM patients carried type κ chain, 27% carried type λ chain, and 65% of symptomatic MM patients had evidence of osteolytic lesions at the X-ray survey. Pelvic bone involvement is present in almost all patients with osteolytic lesions. However, the presence of osteolysis in the biopsied bone area could not be confirmed with certainty because the procedure is not routinely a computed tomography-guided biopsy. Patients' characteristics and drugs used in the treatment regimens are summarized in Supplemental Table S1. In SMM, no significant change in the number of viable osteocytes was observed in histological evaluations carried out after 12 months of observation (median % change: +1.2%, $p = 0.68$, not significative (NS)). The overall response rate of MM patients was 79.3% (nCR/CR 48.3%; VGPR/PR 31%). The mean percent change in osteocyte viability was not correlated with treatment response rates (R2 0.01, p = NS). MM patients treated with BOR-based regimens showed a significantly higher percentage of viable osteocytes compared with controls who were not treated with BOR (% median increase: +6% versus +1.30%; $p = 0.017$) (Fig. 1*A*). On the other hand, no significant difference was observed between patients treated with thalidomide (THAL) or immunomodulatory drugs (IMiDs) and patients who were not treated with those drugs ($p = 0.7$). Patients' treatment with BOR alone showed the most powerful effect in maintaining osteocyte viability compared with treatment without BOR (+14% versus +1.3%, $p = 0.0027$) or with BOR plus DEX (+11.6% versus +4.4%, $p = 0.01$) (Fig. 1*A*).

A multiple regression nonparametric analysis showed that BOR had a significant, positive impact on osteocyte viability ($p = 0.042$), whereas THAL/IMiDs along with ZOL treatments did not show any significant effects ($p = 0.2$). In addition, BOR counterbalanced the negative effect of DEX treatment ($p = 0.035$). Fig. 1*A* shows Gomori's trichrome staining of sections of the iliac crest biopsies, obtained from two representative MM patients treated with BOR; the black arrows indicate viable osteocytes, whereas the white ones indicate empty lacunae.

A reduction of apoptotic osteocytes was observed after 12 months in MM patients treated with a BOR-based regimen (median % of apoptotic osteocytes: PRE 10% versus POST 3%; $p = 0.0085$) compared with MM patients treated without BOR (median % of apoptotic osteocytes post-treatment: BOR+ 3% versus BOR– 13%; $p = 0.032$) (Fig. 1*B*). The TUNEL assay of the three representative MM patients is shown in Supplemental Fig. S2*A*.

Ex vivo immunofluorescent microscopy for LC3 revealed the staining in both osteocytes and osteoblasts in the bone-BM interface. LC3-positive osteocytes were evaluated inside the bone and not in the BM or on bone surface, as shown in Supplemental Fig. S3*A*. LC3 staining in three representative MM patients is presented in Supplemental Fig. S3*B*. A higher reduction of autophagic osteocytes was observed in MM patients treated with BOR-based regimen compared with those treated without BOR (median % of autophagic osteocytes post-treatment: BOR+ 8.5% versus BOR– 14%; $p = 0.029$) (Fig. 1*C*). A linear regression analysis showed that the treatment with BOR significantly reduced the number of apoptotic osteocytes ($p = 0.025$) and the percentage of autophagic osteocytes ($p = 0.017$). In addition, we found that responding MM patients treated with BOR-based regimen had a significantly higher reduction in the number of autophagic osteocytes compared with MM patients treated without BOR (median % of autophagic osteocytes post-treatment: BOR+ 9% versus BOR– 13%; $p = 0.05$) (data not shown). Data obtained from the histological evaluation of bone biopsies are summarized in Supplemental Table S2.

PIs reduce preosteocyte and osteocyte death induced by human myeloma cell lines (HMCLs)

To understand the mechanisms whereby BOR maintains osteocyte viability in bone from MM patients, we subsequently investigated the in vitro effects of BOR in two different models of MM-induced and DEX-induced osteocyte death. First, we checked whether MM cells or DEX might affect osteocyte differentiation markers in our experimental models. Both HOB-01 and MLO-Y4 cell lines were checked for *FGF23, PHEX, DMP1*, and *SOST* gene expression by real-time PCR. As reported by others, MLO-Y4 cells expressed low to undetectable levels of *DMP1* and *SOST* mRNA,[39] whereas HOB-01 cells were negative for both genes. Both cell lines were negative for *FGF23*. We found the downregulation of *PHEX* both in the cell lines cocultured with RPMI 8226 and in MLO-Y4 after treatment with DEX (Fig. 2).

Thereafter, we showed that BOR alone at 2 nM had a significant positive impact on the viability of both HOB-01 and MLO-Y4 cells after 12 hours of treatment (means % of increase ± standard error (SE) versus control: +9% ± 1% and +11% ± 1%, respectively; $p \leq 0.001$) (Supplemental Fig. S4*A*). A longer exposure to BOR had a negative effect on osteocyte viability. Similar results were observed on both HOB-01 and MLO-Y4 cells when administered with MG 262 at 10 nM (Supplemental Fig. S4*B*). For subsequent experiments, osteocytes were treated with 2 nM BOR that was found to be subapoptotic for HMCLs (data not shown). Second, we found that, as expected, CM of RPMI 8226 (Fig. 3*A*) and JJN3 (Fig. 3*B*) significantly reduced HOB-01 and

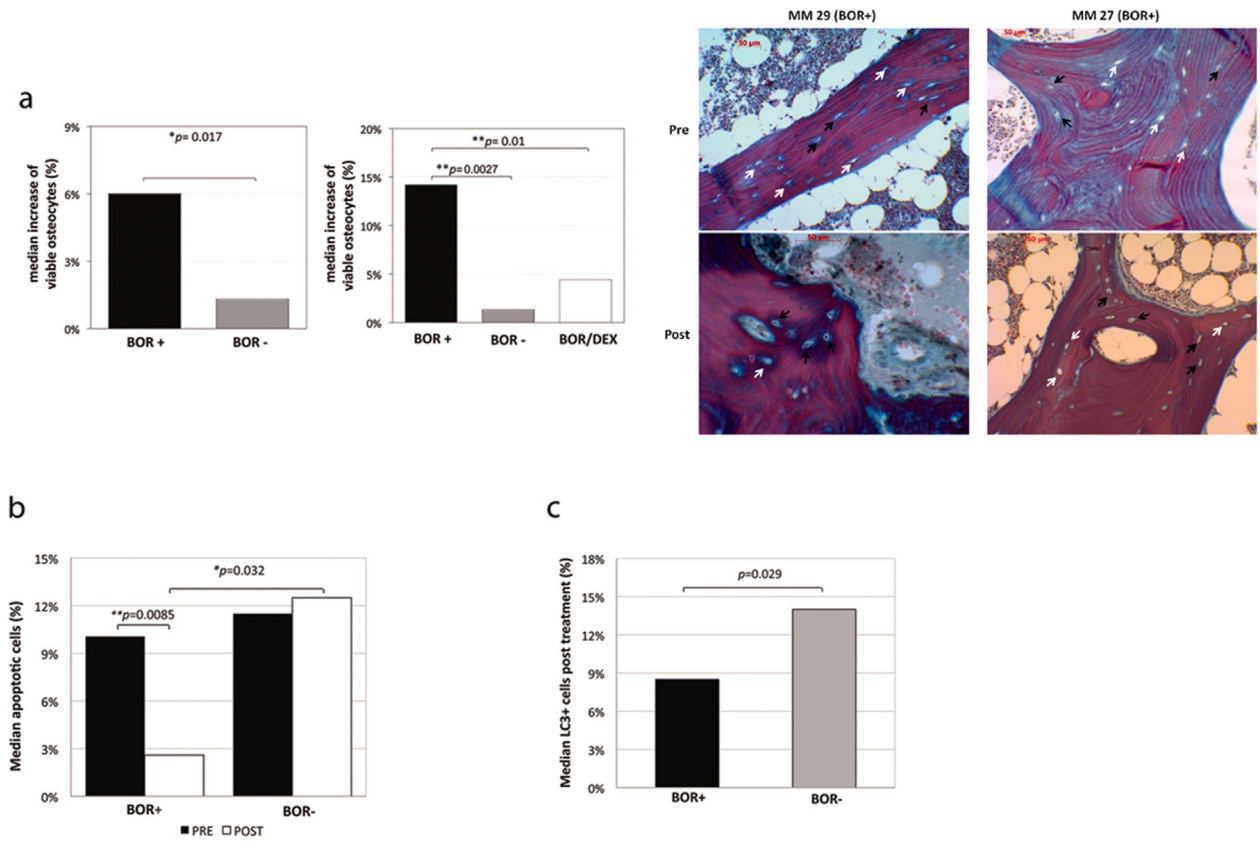

Fig. 1. BOR-based regimen maintains the number of viable osteocytes in MM patients. The number of viable osteocytes was evaluated on bone biopsies of MM patients treated with BOR-based regimen compared with those treated without BOR, and on MM patients treated with BOR alone compared with either patients treated without BOR or patients treated with BOR plus DEX (*A*). Graphs and bars show the median increase of viable osteocytes as evaluated by Gomori's trichrome staining (*A*). Gomori's trichrome staining of sections of the iliac crest biopsy samples, obtained from two representative MM patients treated with BOR (MM 29 and MM 27), pre- (top) and post-(bottom) treatment. MM 29 and MM 27 are responder and nonresponder patients, respectively. Black arrows indicate viable osteocytes and white arrows indicate empty lacunae (*A*). The number of apoptotic osteocytes was evaluated on bone biopsies of MM patients treated with BOR-based regimen compared with those treated without BOR, pre- and post-treatment. Graphs and bars show the median % of apoptotic osteocytes by in situ end labeling (TUNEL) (*B*). The number of autophagic osteocytes (LC3+) was evaluated on bone biopsies of MM patients treated with BOR-based regimen compared with those treated without BOR. Graphs and bars show the median % of autophagic osteocytes by immunofluorescent confocal microscopy (*C*).

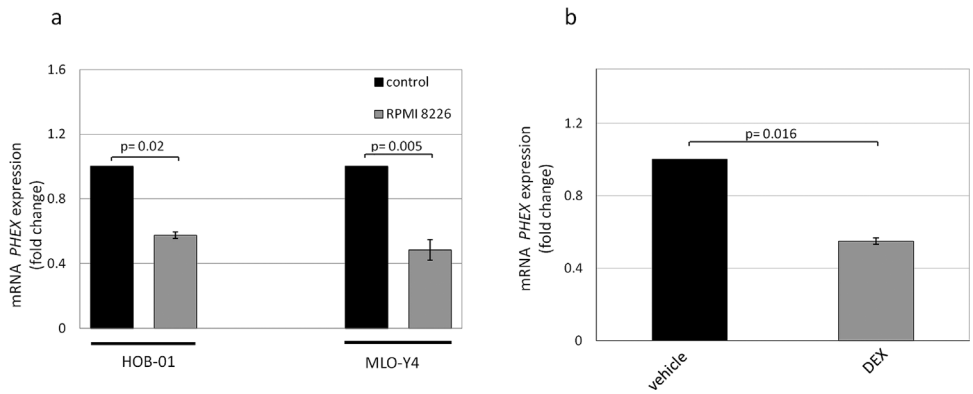

Fig. 2. Effects of RPMI 8226 and DEX on *PHEX* mRNA expression. Both HOB-01 and MLO-Y4 were cocultured with HMCL RPMI 8226 for 48 hours (*A*). MLO-Y4 were treated with DEX (10^{-6} M) for 48 hours or vehicle (*B*). *PHEX* mRNA expression was evaluated by real-time PCR using glyceraldehyde 3-phosphate dehydrogenase (GAPDH) or β-2-microglobulin (β2m) mRNA as internal control. Graphs represent the mean fold change ± SD in the mRNA levels for two independent experiments performed in triplicate.

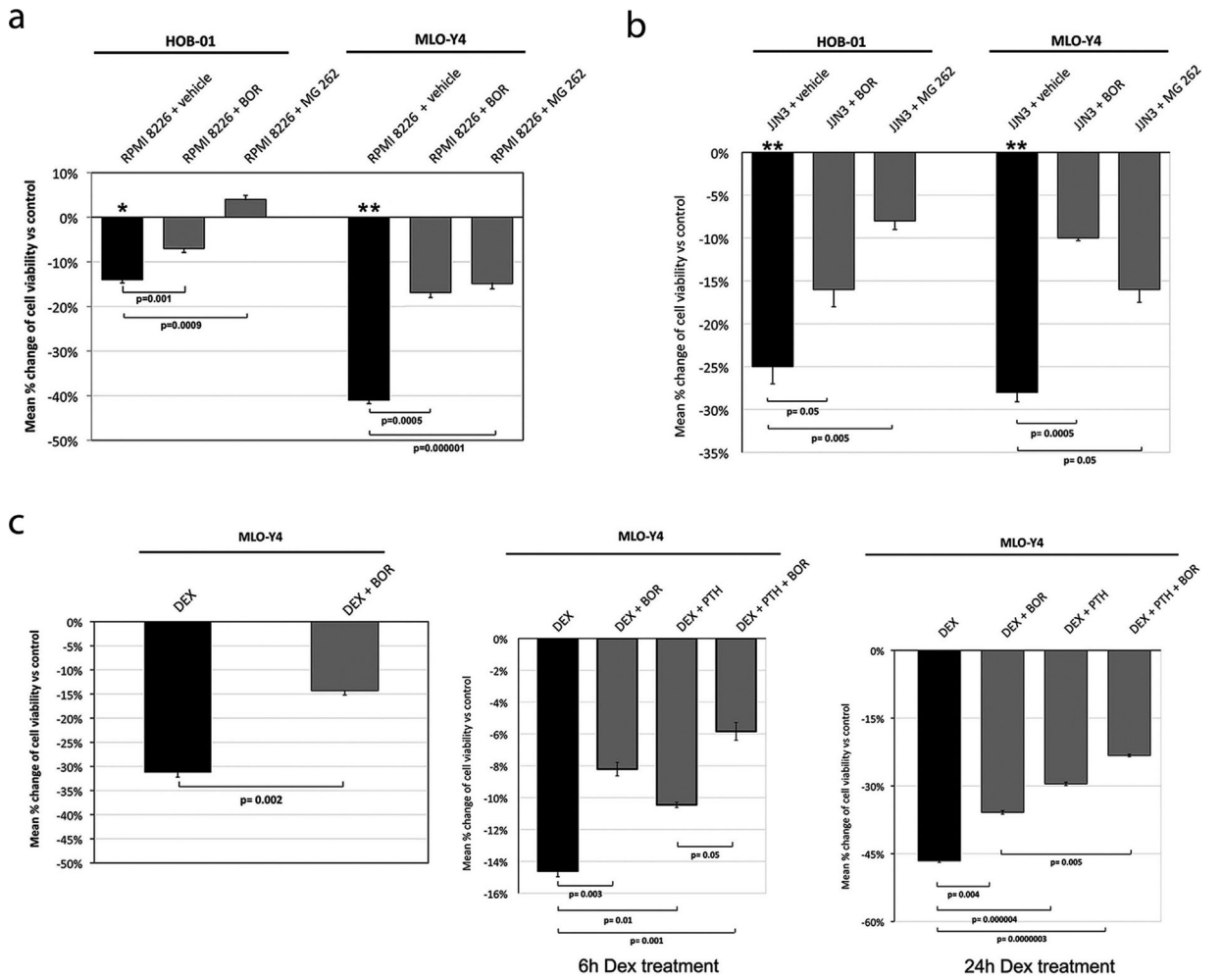

Fig. 3. PIs have positive effect on osteocyte and preosteocyte viability in the presence of HMCLs or DEX treatment. Confluent HOB-01 and MLO-Y4 were incubated with or without the 48-hour CM of HMCLs RPMI 8226 (*A*) or JJN3 (*B*) for 48 hours. Then the culture media was changed and osteocytes were treated with BOR (2 nM) or MG 262 (10 nM) for 12 hours. Confluent MLO-Y4 were also treated with DEX (10^{-6} M) or vehicle for 48 hours. Afterward, the culture media was changed and osteocytes exposed to BOR (2 nM) or vehicle for further 12 hours (*C*). Moreover, MLO-Y4 were incubated with high-dose DEX (10^{-5} M) or vehicle, for 6 hours or 24 hours, to induce cell death. Then the culture media was changed and MLO-Y4 treated with PTH(1-34) (10 nM) for 1 hour or BOR (2 nM) for 12 hours or with the combined treatment PTH(1-34) (1 hour) followed by BOR (12 hours) (*C*). At the end of the culture period, osteocyte viability was assessed by means of colorimetry using tetrazolium salt as described in Materials and Methods. The graphs show the mean % change of cell viability values compared with control ± SE of five independent experiments performed in triplicate. Data were analyzed using two-tailed Student's *t* test. (* and ** = HOB-01 and MLO-Y4 incubated with CM of RPMI 8226 or JJN3 plus vehicle versus control; $^{*}p = 0.001$, $^{**}p < 0.001$)

MLO-Y4 viability (means % of reduction ± SE versus control: RPMI 8226 −14% ± 0.8% and −46% ± 0.9%, respectively; $p \leq 0.001$; JJN3 −25% ± 2% and −28% ± 1.1%, respectively; $p \leq 0.001$). The 12-hour treatment with both PIs BOR and MG 262 significantly reduced the cytotoxic effect on both HOB-01 and MLO-Y4 induced by the CM of either RPMI 8226 (Fig. 3*A*) or JJN3 (Fig. 3*B*). Both the reduction of HOB-01 and MLO-Y4 viability induced by HMCLs and the positive effects of PIs were further confirmed by trypan blue exclusion (Supplemental Fig. S5*A, B*).

PIs blunt DEX-induced osteocyte death, with an enhanced effect in combination with PTH(1-34)

The effect of PIs on DEX-induced osteocyte death was also evaluated using MLO-Y4 because HOB-01 cells did not show any reduction of viability under DEX treatment even at a wide range of concentrations (data not shown). When used at higher doses (10^{-6} M) for 48 hours, DEX was found to significantly reduce MLO-Y4 viability, whereas the addition of 2 nM BOR for 12 hours after DEX treatment significantly reduced the effect of DEX (Fig. 3*C*). Similar results were also obtained with MG 262 (data not shown). Because it is known that PTH(1-34) intermittent administration counteracts the effect of glucocorticoids,[17] we further investigated the potential effect of BOR in combination with PTH(1-34) on DEX-induced osteocyte death. The treatment with BOR (12 hours) or PTH(1-34) (1 hour) alone increased the viability of HOB-01 and MLO-Y4 cells (means % of increase ± SE versus control: BOR +9% ± 1%, $p = 0.02$; +10% ± 1, $p = 0.008$, respectively; PTH: +9% ± 1.2%, $p = 0.02$; +7% ± 1, $p \leq 0.001$, respectively) (data not shown). The combination of BOR and

PTH(1-34) significantly reduced the cytotoxic effect induced either by 6-hour DEX treatment compared with the treatment with PTH(1-34) alone (Fig. 3*C*) or by 24-hour DEX treatment compared with BOR alone (Fig. 3*C*). The reduction of osteocyte viability induced by DEX treatment occurred regardless of the presence or absence of phenol red in the culture media (data not shown).

Autophagic cell death is involved in MM and DEX-induced osteocyte death: effects of PIs

To establish the mechanism by which treatment with PIs blunts both MM and DEX-induced osteocyte death when apoptosis and autophagy are involved, first we checked caspase-3 activation in MLO-Y4 cells. We found that 6-hour treatment with DEX (10^{-6} M) determined the activation of caspase-3, but the subsequent 12-hour treatment with BOR did not affect its activity (Fig. 4*A*). Similar results were also obtained using phenol red-free medium (data not shown). The presence of RPMI 8226 in the coculture transwell system did not affect caspase-3 activity in either HOB-01 (Fig. 4*B*) or MLO-Y4 (Fig. 4*C*) cells and consequently the PIs did not affect caspase-3 activity in either cell line (Fig. 4*B, C*). Similarly, DEX (10^{-6} M) treatment for 48 hours did not affect caspase-3 activity in MLO-Y4 cells (Fig. 4*D*). Similar results were also obtained using phenol red-free medium (Fig. 4*D*).

The potential involvement of autophagy in osteocyte death was then investigated. We found that the treatment with BOR induced LC3 expression, increasing the conversion of LC3I to LC3II compared with the vehicle in both HOB-01 and MLO-Y4 cell lines (Fig. 5*A*). Conversely, we found that, in the coculture system, RPMI 8226 led to an increase of LC3II/I ratio in both HOB-01 and MLO-Y4 cells (Fig. 5*B*), whereas the 12-hour treatment with BOR and MG 262 significantly reduced LC3 expression (Fig. 5*B*). Similarly, MLO-Y4 cells incubated for 48 hours with DEX (10^{-6} M) showed an increased level of LC3 compared with the control blunted by the subsequent 12-hour treatment with both PIs (Fig. 5*C*). A slight induction of LC3 was also founded in both HOB-01 and MLO-Y4 cells when cocultured with lymphoblastic leukemia cell line 697 (Fig. 5*D*). The expression of autophagic marker LC3 was also evaluated by confocal microscopy on the monolayers of MLO-Y4 cells. Accordingly, an increase in the percentage of LC3-positive autophagic osteocytes was observed after 48 hours of coculture with RPMI 8226 (Fig. 6*A*) and DEX treatment (Fig. 6*B*). BOR and MG 262 reduced the percentage of autophagic cells in both systems (Fig. 6*A, B*) (ANOVA $p < 0.001$; Bonferroni $p < 0.05$; Student-Newman-Keuls $p < 0.05$). The TEM examination confirmed the increase of autophagic osteocytes after coculture with RPMI 8226 or treatment with DEX in MLO-Y4 cells (Fig. 6*C*). Furthermore, subsequent treatment with BOR or MG 262 reduced the amount of autophagic osteocytes (Fig. 6*C*). Fig. 6*D* shows high magnification of TEM observations in the same experiments. Concomitantly with the increase of LC3II, the 12-hour treatment with BOR increased the level of p62 level, inhibiting autophagy-dependent degradation in MLO-Y4 cells (Fig. 7*A*); indeed, p62 is the autophagic protein that binds to LC3 and is degraded in autolysosomes by autophagy. Similarly, the presence of RPMI 8226 in a coculture system (Fig. 7*B*) or the treatment of MLO-Y4 cells with DEX (10^{-6} M) (Fig. 7*C*) for 48 hours reduced p62 level. The subsequent 12-hour treatment with BOR was shown to increase their levels (Fig. 7*B, C*).

Finally, for further elucidation of the role of BOR in the autophagic process, MLO-Y4 cell line was pretreated with two different autophagy inhibitors, namely 3-MA (0.5 mM) and CQ (25 μM) or vehicle for 1 hour. They were then exposed to CM of RPMI 8226 (Fig. 8*A*) or DEX (Fig. 8*B*) for further 48 hours followed by BOR treatment. As shown in Fig. 8*A, B*, the presence of autophagy inhibitors blocked the positive effects of BOR on osteocytes viability with a more potent effect of 3-MA on RPMI 8226-treated cells compared with CQ. The same set of experiments was performed in the presence or absence of the caspase-3 inhibitor, Ac-DEVD-CHO (50 nM). The blunted effect of BOR on MLO-Y4 viability was observed either in the presence of HMCLs or after DEX treatment (Fig. 8*C, D*).

Discussion

Among the new drugs used in the treatment of MM patients, PIs including BOR have been demonstrated to stimulate bone formation with a positive effect on bone disease.[29–34] In this study, we found that PIs affect osteocyte and preosteocyte viability, showing a new mechanism of action for this class of drugs.

First, we showed that osteocyte viability was significantly maintained in MM patients treated with BOR-based regimens compared with untreated patients. The potential impact of thalidomide/IMiDs treatment was not conclusive because of the small number of patients treated with IMiDs alone. However, other studies have reported a lack of effect of this type of drugs on osteoblasts and bone formation process.[40,41] BOR is approved for first-line treatment of elderly patients and young patients eligible for high-dose therapy, and it is also approved as second-line therapy for relapsed/refractory patients.[42] The use of BOR in combination with or without steroid and/or alkylating agents and/or IMiDs is preferred but not mandatory in patients with high-risk cytogenetic disease associated with poor prognosis and high bone disease.

The ex vivo analysis of both osteocyte apoptosis and autophagy in bone biopsies of MM patients indicated a reduction in both processes after treatment with BOR. We can suppose that both a direct effect of PIs on osteocytes as well as an indirect PTH-mediated one could occur in vivo in MM patients treated with BOR. Other studies have demonstrated that treatment with BOR determines a significant and reproducible pulsatile increase of serum PTH in responding MM patients,[43] supporting the hypothesis that the anabolic effect of BOR may be mediated at least in part by PTH, which is known to be able to affect osteocyte apoptosis.[17,19] In our cohort of MM patients, the effect of BOR on osteocyte viability was irrespective of the response to treatment, suggesting that the direct effect is likely to be predominant compared with the indirect one. However, we cannot exclude their in vivo coexistence.

To understand the mechanisms underlying the in vivo effect of BOR on osteocyte viability, we checked the potential in vitro effects of PIs on osteocyte survival. Two different in vitro models were used: 1) MM cell-induced osteocyte death, and 2) drug-induced osteocyte death with high-dose DEX. In both systems, we demonstrated a reduction in the rate of preosteocyte and osteocyte death caused by PIs. These effects were observed at lower concentrations of BOR compared with those able to stimulate osteogenic differentiation of mesenchymal cells[30] and are subapoptotic for MM cells. BOR can also potentiate the stimulatory effect of PTH(1-34) on osteocyte viability after DEX treatment. Interestingly, daily PTH administration in MM mouse

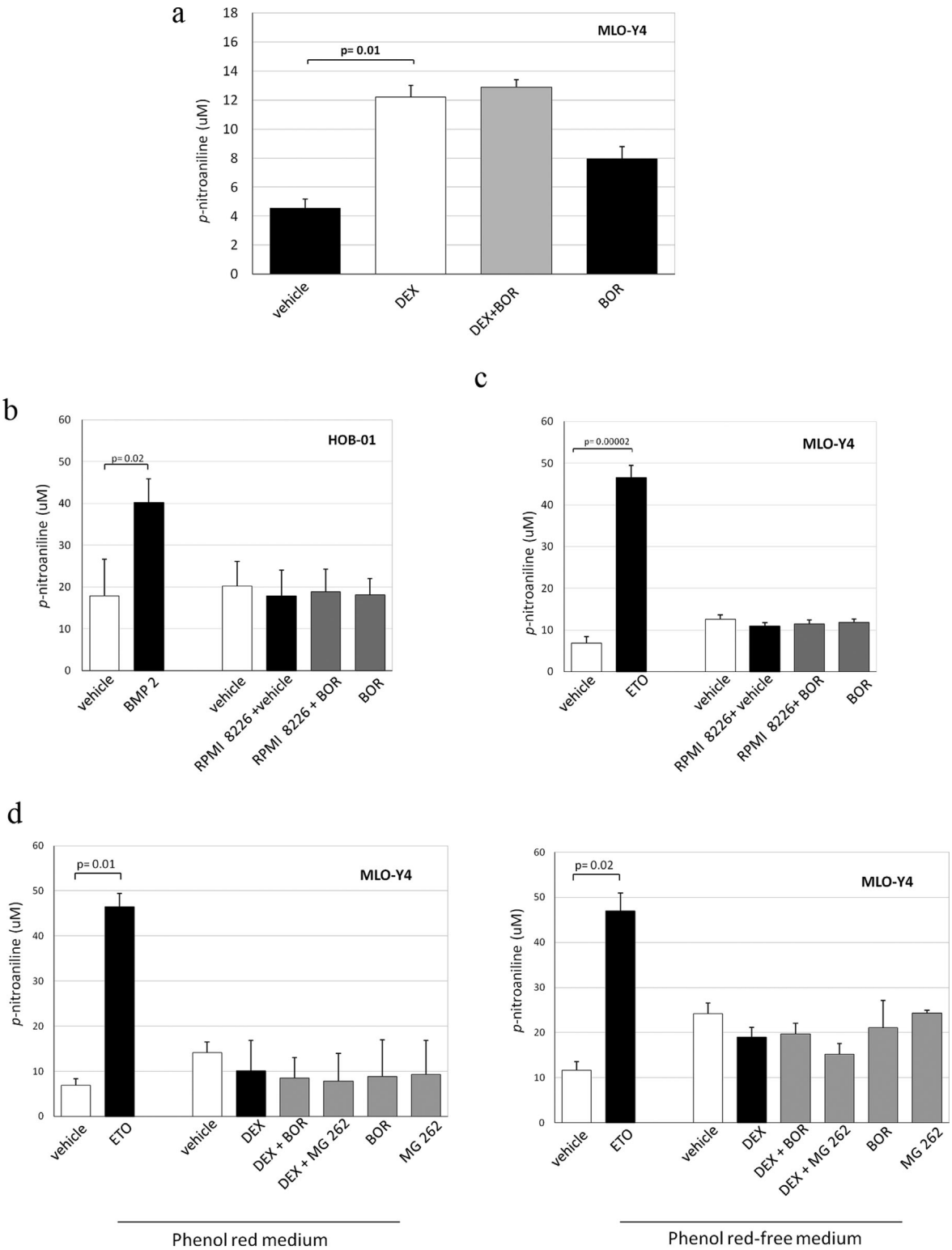

Fig. 4. Lack of effect of HMCLs and proteasome inhibitors on the activity of the apoptotic marker caspase-3 in osteocytes. MLO-Y4 were treated with DEX 10^{-6} M for 6 hours and then incubated with BOR (2 nM) or vehicle for 12 hours (*A*). HOB-01 (*B*) and MLO-Y4 (*C*) were cocultured with HMCL RPMI 8226 in the presence or absence of BOR (2 nM) or vehicle. MLO-Y4 were treated with DEX 10^{-6} M for 48 hours in the presence or absence of BOR (2 nM), MG 262 (10 nM) or vehicle in both phenol red and phenol red-free medium (*D*). Both nonadherent and adherent cells were harvested, combined, and analyzed for caspase-3 activity. The graphs show the concentration of chromophore p-nitroaniline related to caspase-3 activity, as described in Materials and Methods. The data represent the mean value ± SD of four independent experiments. HOB-01 treated with BMP-2 200 ng/mL for 6 hours and MLO-Y4 treated with etoposide (ETO) 50 uM for 24 hours were used as positive controls. Data were analyzed using two-tailed Student's *t* test.

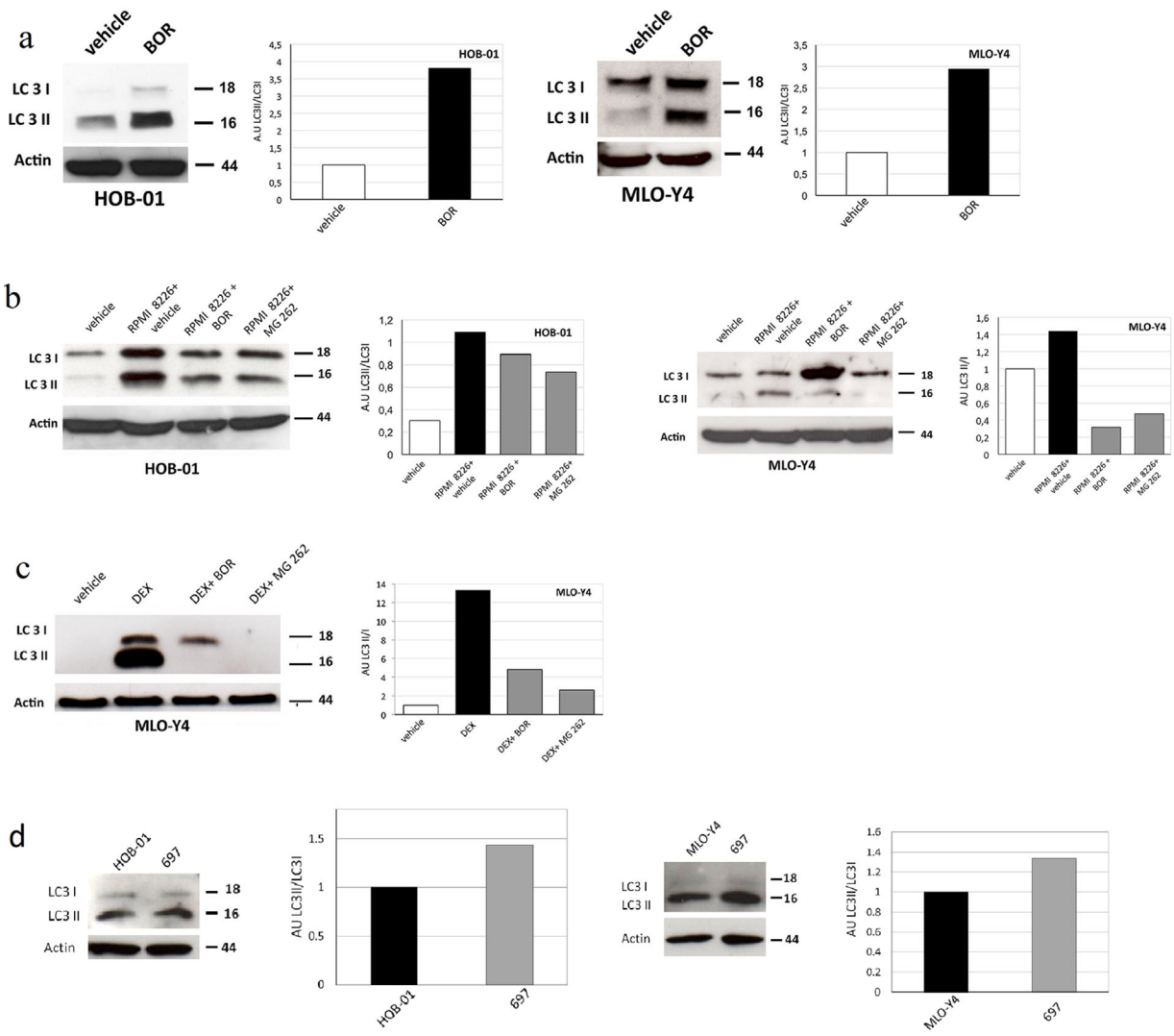

Fig. 5. PIs increase the expression of the autophagy marker LC3 by preosteocytes and osteocytes, while blunting the upregulation induced by HMCL and DEX treatment. Both HOB-01 and MLO-Y4 were treated with BOR (2 nM) or vehicle for 12 hours (*A*). Both HOB-01 and MLO-Y4 were cocultured with RPMI 8226 for 48 hours and then treated with BOR (2 nM) or MG 262 (10 nM) or vehicle for 12 hours (*B*). MLO-Y4 were incubated with DEX 10^{-6} M or vehicle for 48 hours and then treated with BOR (2 nM) or MG 262 (10 nM) or vehicle for 12 hours (*C*). HOB-01 and MLO-Y4 were cocultured with the lymphoblastic leukemia cell line 697 for 48 hours in the presence of a transwell insert (*D*). LC3 protein level was evaluated by means of Western blot. Graphs show the LC3II/LC3I ratio normalized for the internal control Actin level relative to vehicle treatment.

models has been reported to increase osteoblast formation and bone mass and consequently reduce the tumoral burden.[44] Our data showed that the positive effect of BOR on DEX-induced osteocyte death was enhanced when combined with a PTH(1-34) short-term treatment compared with treatment with BOR and PTH(1-34) alone. PTH receptor signaling has been recently reported to mediate the anti-myeloma effect of PIs, including BOR.[45]

The mechanisms involved in MM-induced osteocyte death and the protective effect of PIs on osteocyte survival were further investigated. First, we found that autophagic death rather than apoptosis was involved in our experimental model, in either human preosteocytes or murine osteocytes, as shown by both the increased expression of the autophagy marker LC3II by Western blot and confocal microscopy and the lack of effect on caspase-3 activation and APAF-1 expression. Moreover, both treatment with DEX and the presence of MM cells reduced the protein level of p62, a key player in the selective autophagic degradation of many proteins.[46]

Further studies will be necessary to identify factors produced by MM cells that may activate autophagic osteocyte death. TNF-alpha was reported to induce apoptosis but not autophagy in osteocytes.[26] Accordingly, we previously reported that anti-TNF-alpha antibody failed to block MM cell-induced osteocyte death.[28] Recent data reported that direct cell-to-cell interactions between osteocytes and MM cells upregulate SOST in osteocytes;[47] however, there is no evidence in support of SOST inducing autophagy in osteocytes.

Growing evidence underlines the role of autophagy in the regulation of osteocyte survival and consequently in the control of skeletal homeostasis and bone remodeling.[48] A suppression of the basal level of autophagy has been reportedly associated with

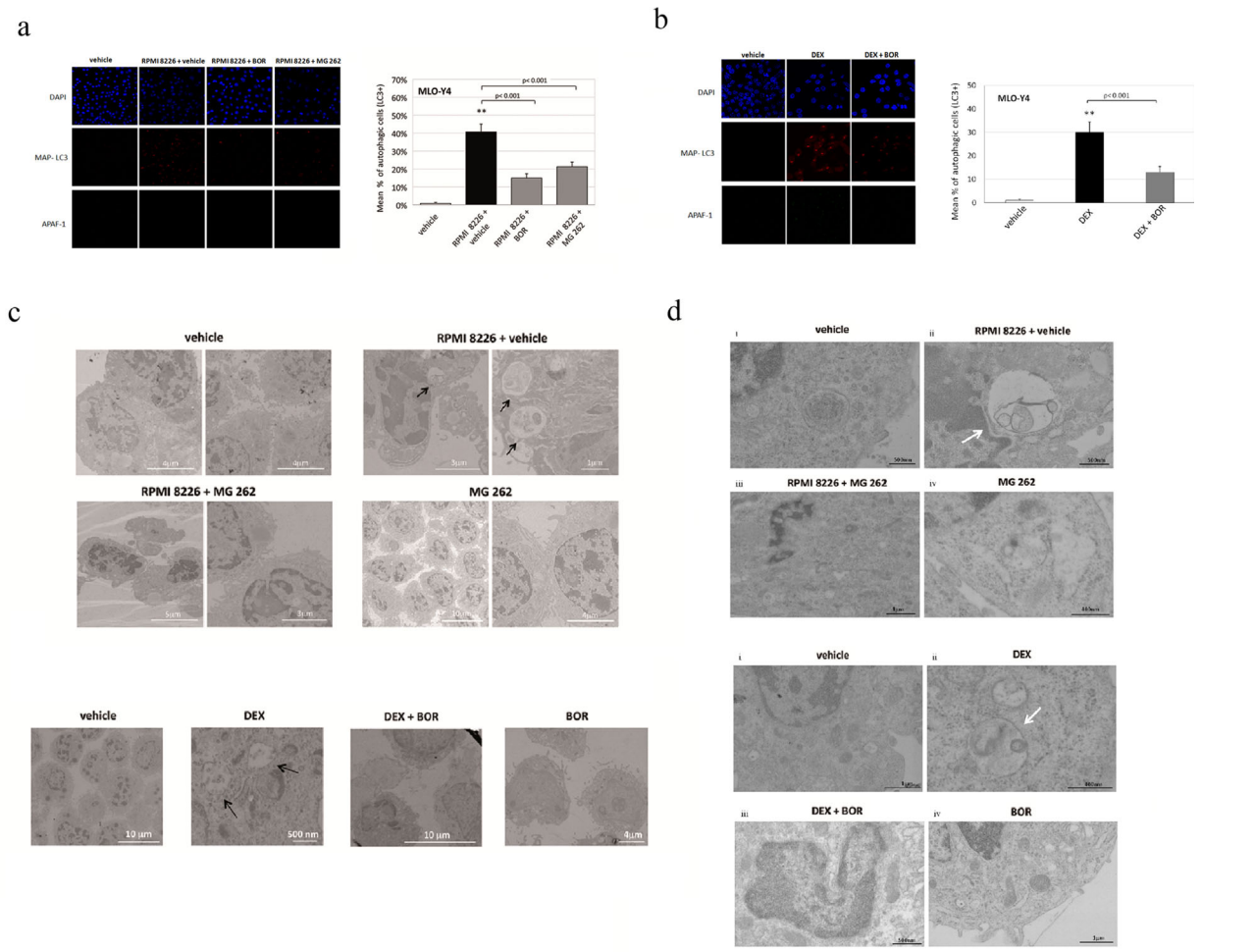

Fig. 6. Confocal and transmission electron microscopy reveal that PIs blunt HMCL and DEX-induced autophagic death in MLOY4. Osteocyte autophagy was assessed by immunofluorescent confocal microscopy as described in Materials and Methods. Confluent MLO-Y4 were cocultured for 48 hours with or without RPMI 8226 in the presence of transwell insert and then treated for 12 hours with BOR (2 nM), MG 262 (10 nM), or vehicle (*A*). Confluent MLO-Y4 were also incubated with DEX 10^{-6} M for 48 hours and then treated with BOR (2 nM) or vehicle for 12 hours (*B*). The graphs show the mean % ± SD of MAP LC3-positive osteocytes for each condition. Original magnification 40×. DAPI (blue) for nuclei; MAP-LC3 (red) for autophagy. Data were analyzed by ANOVA followed by Bonferroni and Student-Newman-Keuls tests (** = MLO-Y4 incubated with RPMI 8226 or treated with DEX plus vehicle versus vehicle; ANOVA $p < 0.001$; Student-Newman-Keuls $p < 0.05$; Bonferroni $p < 0.05$). Osteocyte autophagy was assessed by transmission electron microscopy as described in Materials and Methods. MLO-Y4 were cocultured for 48 hours with or without RPMI 8226 in the presence of transwell insert and then treated for 12 hours with MG 262 (10 nM) or vehicle (*C*). Confluent MLO-Y4 were treated for 48 hours with or without DEX 10^{-6} M or vehicle and then treated for 12 hours with BOR (2 nM) or vehicle (*C*). TEM micrographs show cell ultrastructure. The arrows indicate autophagic cells. High magnification of TEM observations of the monolayer of MLO-Y4 cells cocultured for 48 hours with RPMI 8226 in a transwell insert and then treated with MG 262 (10 nM) or vehicle. Confluent MLO-Y4 were treated for 48 hours with or without DEX 10^{-6} M or vehicle and then treated for 12 hours with BOR (2 nM) or vehicle (*D*). Representative micrographs show cells with normal ultrastructure (i, iii, iv) and cells with autophagic vacuoles (ii). White arrows indicate cells with autophagic vacuoles.

aging-related bone changes;[25] on the other hand, an increase in both osteocyte and osteoblast autophagic death was reported in glucocorticoid treatments characterized by rapid bone loss.[13,15] Similarly, higher-dose DEX treatment was found to have triggered autophagic markers in osteocytes.[26] In the present study, we report the involvement of autophagy in MM-induced osteocyte death and related bone remodeling alterations. Recently, impaired osteoblastogenesis in osteogenesis imperfecta has been reported to be related to an upregulation of autophagy.[49] This evidence suggests that bone cells' autophagy could be a potential target in the bone microenvironment.

The role of BOR in regulating autophagy has recently been reported in different cell types.[50–54] In line with these data, we found that BOR can increase the level of LC3II/I ratio and block the degradation of p62 in MLO-Y4 cells, indicating the ability to target the autophagic pathway. BOR's capability to inhibit autophagy was also demonstrated by TEM examinations. Furthermore, we also found that the use of autophagy inhibitors blunted the positive effects of BOR on MLO-Y4 viability. Interestingly, we found that BOR increased LC3I in RPMI 8226-treated osteocytes, whereas it decreased LC3I in DEX-treated cells. This suggests that osteocytes are likely to respond

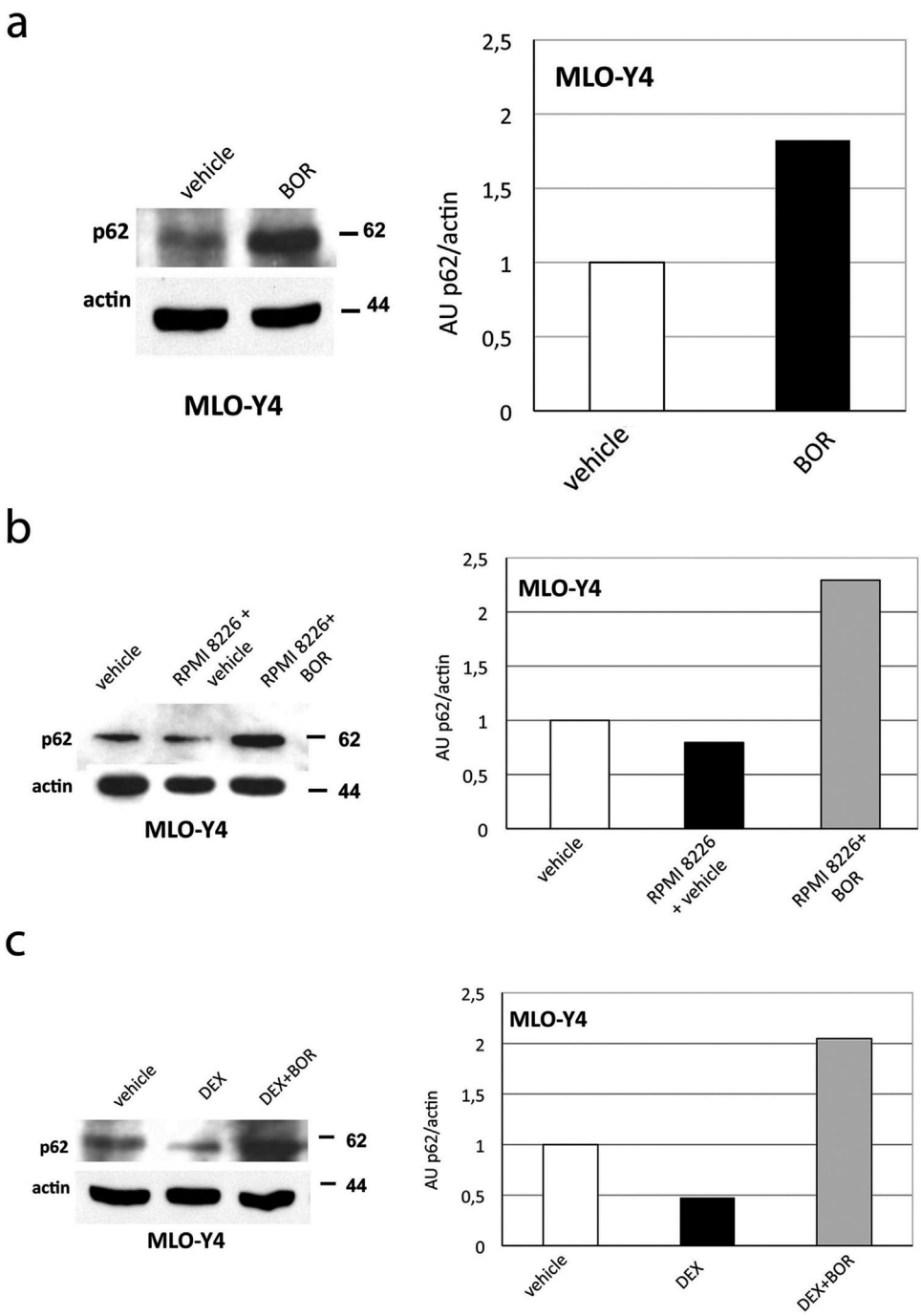

Fig. 7. BOR blocks p62 degradation during autophagic death in MLO-Y4. MLO-Y4 were treated with BOR (2 nM) or vehicle for 12 hours (*A*), or cocultured with RPMI 8226 (*B*) or incubated with DEX 10^{-6} M or vehicle (*C*) for 48 hours and then treated with BOR (2 nM) or vehicle for 12 hours. p62 protein level was evaluated by means of Western blot. Graphs show the p62 level normalized for the internal control Actin level relative to vehicle treatment. Pictures and graphs show a representative experiment performed independently twice.

differently to stress induced by MM cells and by DEX treatment, respectively. On the other hand, the effect of BOR on LC3II was the same in both MM-induced and DEX-induced autophagy. Consistently, LC3II is known to be the main protein involved in the autophagosome formation.[46,55,56]

Although we did not find the activation of apoptosis in either osteocytes or preosteocytes in our coculture transwell system or upon DEX treatment, we cannot exclude the role of apoptosis or the connection between autophagy and apoptotic pathways, having shown the blocking effect of caspase-3 inhibitor on the positive effects of BOR in vitro. It is likely that apoptosis may occur as a flow from apoptosis to autophagy. Consistently, other researchers reported that MM cells induce apoptosis in murine preosteocytic cell line MLO-A5.[57]

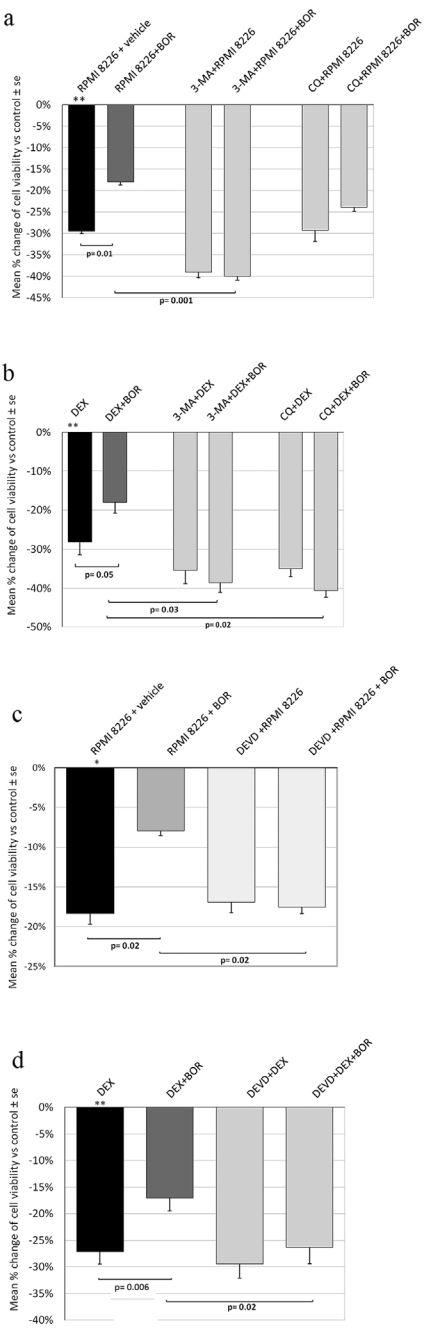

Fig. 8. Effect of autophagic and apoptotic inhibitors on MLO-Y4 viability. Confluent MLO-Y4 were incubated with 3-MA (0.5 mM) or CQ (25 μM) or vehicle for 1 hour before addition of 48-hour CM of the HMCL RPMI 8226 (*A*) or DEX (10^{-6} M) (*B*) or vehicle for 48 hours. Moreover, MLO-Y4 were incubated with Ac-DEVD-CHO (50 nM) or vehicle for 1 hour before addition of 48-hour CM of the HMCL RPMI 8226 (*C*) or DEX (10^{-6} M) (*D*) or vehicle for 48 hours. Then the culture media was changed and osteocytes were treated with BOR (2 nM) or vehicle for 12 hours. At the end of the culture period, osteocyte viability was assessed by means of colorimetry using tetrazolium salt, as described in Materials and Methods. Autophagy inhibitors were maintained for the entire culture period. Graphs show the mean % change of cell viability values compared with control ± SE of three independent experiments performed in triplicate. Data were analyzed using two-tailed Student's *t* test. (Control = MLO-Y4 incubated with vehicle; ** = MLO-Y4 incubated with CM of RPMI 8226 or DEX plus vehicle versus control; $^{**}p < 0.001$)

In conclusion, our data identified osteocyte autophagy as a potential target in MM bone disease and suggested that PIs lead to an increase in osteocyte viability through autophagy modulation and improved bone integrity in MM patients.

Disclosures

All authors state that they have no conflicts of interest.

Acknowledgments

We thank Dirce Gennari for her technical support.

This work was supported in part by a grant from the Associazione Italiana per la Ricerca sul Cancro (AIRC): Special Program in Molecular Clinical Oncology 5 × 1000 n° 9965 (NG) and IG2014 n° 15531 (NG); a fellowship from the "Consorzio Spinner"; and a fellowship FIRC Elda e Attilio Pandolfi ID 16462 (DT).

Authors' roles: Study design: NG. Experimental conduct: DT, MB, VM, VF, and FC. Histological analysis using confocal microscopy and evaluation of osteocyte viability on bone biopsies: CP, PS, and MF. Data collection, analysis, and interpretation: DT and NG. Clinical data and patients: BDP, LC, FA, and FA. Histological analysis of bone biopsies: EM and CM. Manuscript preparation: NG and DT. Approving final version of the manuscript: all authors. NG takes responsibility for the integrity of the data analysis.

References

1. Roodman GD. Pathogenesis of myeloma bone disease. Leukemia. 2009;23(3):435–41.
2. Giuliani N, Rizzoli V, Roodman GD. Multiple myeloma bone disease: pathophysiology of osteoblast inhibition. Blood. 2006; 108(13):3992–6.
3. Bonewald LF. The amazing osteocyte. J Bone Miner Res. 2011; 26(2):229–38.
4. Heino TJ, Hentunen TA. Differentiation of osteoblasts and osteocytes from mesenchymal stem cells. Curr Stem Cell Res Ther. 2008;3(2):131–45.
5. Noble BS, Reeve J. Osteocyte function, osteocyte death and bone fracture resistance. Mol Cell Endocrinol. 2000;159(1–2):7–13.
6. Palumbo C, Palazzini S, Marotti G. Morphological study of intercellular junctions during osteocyte differentiation. Bone. 1990;11(6):401–6.
7. Teti A, Zallone A. Do osteocytes contribute to bone mineral homeostasis? Osteocytic osteolysis revisited. Bone. 2009;44(1):11–6.
8. van Bezooijen RL, ten Dijke P, Papapoulos SE, Lowik CW. SOST/sclerostin, an osteocyte-derived negative regulator of bone formation. Cytokine Growth Factor Rev. 2005;16(3):319–27.
9. Chen H, Senda T, Kubo KY. The osteocyte plays multiple roles in bone remodeling and mineral homeostasis. Med Mol Morphol. 2015; 48(2):61–8.
10. Weinstein RS, Nicholas RW, Manolagas SC. Apoptosis of osteocytes in glucocorticoid-induced osteonecrosis of the hip. J Clin Endocrinol Metab. 2000;85(8):2907–12.
11. Tomkinson A, Reeve J, Shaw RW, Noble BS. The death of osteocytes via apoptosis accompanies estrogen withdrawal in human bone. J Clin Endocrinol Metab. 1997;82(9):3128–35.
12. Emerton KB, Hu B, Woo AA, et al. Osteocyte apoptosis and control of bone resorption following ovariectomy in mice. Bone. 2010; 46(3):577–83.
13. O'Brien CA, Jia D, Plotkin LI, et al. Glucocorticoids act directly on osteoblasts and osteocytes to induce their apoptosis and reduce bone formation and strength. Endocrinology. 2004;145(4):1835–41.
14. Canalis E, Delany AM. Mechanisms of glucocorticoid action in bone. Ann NY Acad Sci. 2002;966:73–81.

15. Lane NE, Yao W, Balooch M, et al. Glucocorticoid-treated mice have localized changes in trabecular bone material properties and osteocyte lacunar size that are not observed in placebo-treated or estrogen-deficient mice. J Bone Miner Res. 2006;21(3):466–76.
16. Tatsumi S, Ishii K, Amizuka N, et al. Targeted ablation of osteocytes induces osteoporosis with defective mechanotransduction. Cell Metab. 2007;5(6):464–75.
17. Weinstein RS, Jilka RL, Almeida M, Roberson PK, Manolagas SC. Intermittent parathyroid hormone administration counteracts the adverse effects of glucocorticoids on osteoblast and osteocyte viability, bone formation, and strength in mice. Endocrinology. 2010;151(6):2641–9.
18. Keller H, Kneissel M. SOST is a target gene for PTH in bone. Bone. 2005;37(2):148–58.
19. Jilka RL, Weinstein RS, Bellido T, Roberson P, Parfitt AM, Manolagas SC. Increased bone formation by prevention of osteoblast apoptosis with parathyroid hormone. J Clin Invest. 1999;104(4):439–46.
20. Plotkin LI, Weinstein RS, Parfitt AM, Roberson PK, Manolagas SC, Bellido T. Prevention of osteocyte and osteoblast apoptosis by bisphosphonates and calcitonin. J Clin Invest. 1999;104(10):1363–74.
21. Plotkin LI, Manolagas SC, Bellido T. Dissociation of the pro-apoptotic effects of bisphosphonates on osteoclasts from their anti-apoptotic effects on osteoblasts/osteocytes with novel analogs. Bone. 2006; 39(3):443–52.
22. Pengo N, Scolari M, Oliva L, et al. Plasma cells require autophagy for sustainable immunoglobulin production. Nat Immunol. 2013;14(3): 298–305.
23. Srinivas V, Bohensky J, Zahm AM, Shapiro IM. Autophagy in mineralizing tissues: microenvironmental perspectives. Cell Cycle. 2009;8(3):391–3.
24. Tsujimoto Y, Shimizu S. Another way to die: autophagic programmed cell death. Cell Death Differ. 2005;12(Suppl 2):1528–34.
25. Onal M, Piemontese M, Xiong J, et al. Suppression of autophagy in osteocytes mimics skeletal aging. J Biol Chem. 2013;288(24):17432–40.
26. Xia X, Kar R, Gluhak-Heinrich J, et al. Glucocorticoid-induced autophagy in osteocytes. J Bone Miner Res. 2010;25(11):2479–88.
27. Yao W, Dai W, Jiang JX, Lane NE. Glucocorticoids and osteocyte autophagy. Bone. 2013;54(2):279–84.
28. Giuliani N, Ferretti M, Bolzoni M, et al. Increased osteocyte death in multiple myeloma patients: role in myeloma-induced osteoclast formation. Leukemia. 2012;26(6):1391–401.
29. Garrett IR, Chen D, Gutierrez G, et al. Selective inhibitors of the osteoblast proteasome stimulate bone formation in vivo and in vitro. J Clin Invest. 2003;111(11):1771–82.
30. Giuliani N, Morandi F, Tagliaferri S, et al. The proteasome inhibitor bortezomib affects osteoblast differentiation in vitro and in vivo in multiple myeloma patients. Blood. 2007;110(1):334–8.
31. Zangari M, Esseltine D, Lee CK, et al. Response to bortezomib is associated to osteoblastic activation in patients with multiple myeloma. Br J Haematol. 2005;131(1):71–3.
32. Shimazaki C, Uchida R, Nakano S, et al. High serum bone-specific alkaline phosphatase level after bortezomib-combined therapy in refractory multiple myeloma: possible role of bortezomib on osteoblast differentiation. Leukemia. 2005;19(6):1102–3.
33. Heider U, Kaiser M, Muller C, et al. Bortezomib increases osteoblast activity in myeloma patients irrespective of response to treatment. Eur J Haematol. 2006;77(3):233–8.
34. Zangari M, Yaccoby S, Cavallo F, Esseltine D, Tricot G. Response to bortezomib and activation of osteoblasts in multiple myeloma. Clin Lymphoma Myeloma. 2006;7(2):109–14.
35. Bodine PV, Vernon SK, Komm BS. Establishment and hormonal regulation of a conditionally transformed preosteocytic cell line from adult human bone. Endocrinology. 1996;137(11):4592–604.
36. Bonewald LF. Establishment and characterization of an osteocyte-like cell line, MLO-Y4. J Bone Miner Metab. 1999;17(1):61–5.
37. Rosser J, Bonewald LF. Studying osteocyte function using the cell lines MLO-Y4 and MLO-A5. Methods Mol Biol. 2012;816:67–81.
38. Sena P, Manfredini G, Benincasa M, et al. Up-regulation of the chemo-attractive receptor ChemR23 and occurrence of apoptosis in human chondrocytes isolated from fractured calcaneal osteochondral fragments. J Anat. 2014;224(6):659–68.
39. Yang W, Harris MA, Heinrich JG, Guo D, Bonewald LF, Harris SE. Gene expression signatures of a fibroblastoid preosteoblast and cuboidal osteoblast cell model compared to the MLO-Y4 osteocyte cell model. Bone. 2009;44(1):32–45.
40. Terpos E, Christoulas D, Kastritis E, et al. The combination of lenalidomide and dexamethasone reduces bone resorption in responding patients with relapsed/refractory multiple myeloma but has no effect on bone formation: final results on 205 patients of the Greek myeloma study group. Am J Hematol. 2014;89(1):34–40.
41. Munemasa S, Sakai A, Kuroda Y, et al. Osteoprogenitor differentiation is not affected by immunomodulatory thalidomide analogs but is promoted by low bortezomib concentration, while both agents suppress osteoclast differentiation. Int J Oncol. 2008;33(1):129–36.
42. Engelhardt M, Terpos E, Kleber M, et al. European Myeloma Network recommendations on the evaluation and treatment of newly diagnosed patients with multiple myeloma. Haematologica. 2014;99(2):232–42.
43. Zangari M, Yaccoby S, Pappas L, et al. A prospective evaluation of the biochemical, metabolic, hormonal and structural bone changes associated with bortezomib response in multiple myeloma patients. Haematologica. 2011;96(2):333–6.
44. Pennisi A, Ling W, Li X, et al. Consequences of daily administered parathyroid hormone on myeloma growth, bone disease, and molecular profiling of whole myelomatous bone. PLoS One. 2010;5(12):e15233.
45. Zangari M, Berno T, Yang Y, et al. Parathyroid hormone receptor mediates the anti-myeloma effect of proteasome inhibitors. Bone. 2014;61:39–43.
46. Jiang P, Mizushima N. LC3- and p62-based biochemical methods for the analysis of autophagy progression in mammalian cells. Methods. 2015;75:13–8.
47. Calle JD, Bellido T, Roodman GDD. Direct cell-to-cell interactions between osteocytes and multiple myeloma (MM) cells upregulate Sost and downregulate OPG expression in osteocytes: evidence for osteocytic contributions to MM-induced bone disease. Blood. 2013;122(21):1.
48. Hocking LJ, Whitehouse C, Helfrich MH. Autophagy: a new player in skeletal maintenance? J Bone Miner Res. 2012;27(7):1439–47.
49. Gioia R, Panaroni C, Besio R, et al. Impaired osteoblastogenesis in a murine model of dominant osteogenesis imperfecta: a new target for osteogenesis imperfecta pharmacological therapy. Stem Cells. 2012;30(7):1465–76.
50. Selimovic D, Porzig BB, El-Khattouti A, et al. Bortezomib/proteasome inhibitor triggers both apoptosis and autophagy-dependent pathways in melanoma cells. Cell Signal. 2013;25(1):308–18.
51. Auner HW, Cenci S. Recent advances and future directions in targeting the secretory apparatus in multiple myeloma. Br J Haematol. 2015;168(1):14–25.
52. Periyasamy-Thandavan S, Jackson WH, Samaddar JS, et al. Bortezomib blocks the catabolic process of autophagy via a cathepsin-dependent mechanism, affects endoplasmic reticulum stress and induces caspase-dependent cell death in antiestrogen-sensitive and resistant ER+ breast cancer cells. Autophagy. 2010;6(1):19–35.
53. Hui B, Shi YH, Ding ZB, et al. Proteasome inhibitor interacts synergistically with autophagy inhibitor to suppress proliferation and induce apoptosis in hepatocellular carcinoma. Cancer. 2012;118(22):5560–71.
54. Kao C, Chao A, Tsai CL, et al. Bortezomib enhances cancer cell death by blocking the autophagic flux through stimulating ERK phosphorylation. Cell Death Dis. 2014;5: e1510.
55. Kabeya Y, Mizushima N, Ueno T, et al. LC3, a mammalian homologue of yeast Apg8p, is localized in autophagosome membranes after processing. EMBO J. 2000;19(21):5720–8.
56. Tanida I, Ueno T, Kominami E. LC3 conjugation system in mammalian autophagy. Int J Biochem Cell Biol. 2004;36(12):2503–18.
57. Delgado-Calle J, Anderson J, Plotkin LI, Bellido T, Roodman GD. Notch- and TNF alpha-activated signaling pathways mediate osteocyte apoptosis triggered by multiple myeloma cells. Blood. 2014;124(21):3.